Analysis of the Synthesis of Ultrafine AlN Powders in an Induction Plasma Reactor

Jean-Francois Bilodeau[1,2], Pierre Proulx[1]

[1] Département de Génie Chimique,
Université de Sherbrooke
Sherbrooke (Québec) Canada J1K 2R1

[2] Now at Centre de Physique des Plasmas et Applications de Toulouse,
U.R.A. C.N.R.S. nº 277, Université Paul Sabatier,
118 Route de Narbonne, 31062 Toulouse, France

A two-dimensional model is developed for the synthesis of aluminum nitride powders by the reaction between aluminum and ammonia in an induction plasma reactor. Plasma-particle interactions are considered in the induction zone where coarser particles heat up and evaporate. Aluminum particle formation and growth occur by homogeneous nucleation, surface diffusion and Brownian coagulation. Thermophoresis and Brownian diffusion are considered. A simple heterogeneous mechanism is proposed for the nitridation of aluminum by ammonia. The model allows for solutions in arbitrary, recirculating flows. The variables describing the operation of the reactor and the characteristics of the powder are presented. Within the range studied, increasing the quench flowrate leads to a lower exit mean number diameter and higher yield of nitridation.

1. Introduction

The high thermal conductivity and electrical resistivity of aluminum nitride make it an attractive material for the electronics industry (1). Sintering requires the synthesis of powders of fine granulometry and high purity (2). The thermal conductivity of the final product is also highly sensitive to the presence of oxygen (2,3). Thermal plasmas are of particular interest to meet these requirements and many studies have been conducted for AlN synthesis in such processes, using various reactants and configurations (1-9).

A two-dimensional model is described simulating the growth, transport and nitridation mechanisms for the synthesis of aluminum nitride. It is applied to the case of a reactor made from an induction plasma torch and a wider reaction chamber downstream, as schematized in Figure 1. Relatively coarse (> 1 mm) aluminum powders are injected axially and evaporated in the high temperature zone near the induction coil. Ammonia is injected in the reaction zone, increasing the cooling and reacting with the condensed aluminum. The fields characterizing the operation of the reactor (temperature, stream function, fraction of ammonia) and powder properties (number concentration, mean diameter, nitridation yield) are analyzed. The effect of the quench flowrate on exit powder properties is estimated.

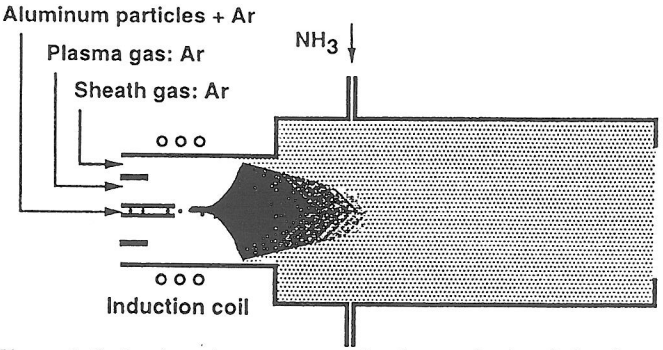

Figure 1. Induction plasma reactor for the synthesis of aluminum nitride

2. Model:

The reactor is modelled in two separate sections. In the first one the gas velocity, temperature and aluminum vapor concentration fields are solved in the induction tube, considering interactions with the coarser particles injected. The second model solves for the same fields, and additionally for ammonia concentration and particle growth, transport and nitridation. This model uses as entrance conditions the velocities, temperatures and concentrations estimated by the first model.

Velocities, temperature, ammonia and metal vapor concentration:

The two-dimensional equations of continuity, axial and radial momentum, and metal vapor concentration are solved as described by Proulx et al (10) in the case of high particle loading. The two-dimensional electromagnetic fields are solved as given by Mostaghimi et al (11). The main assumptions and characteristics of the solution are:

- Steady, laminar ($Re < 200$), axisymmetric flow in local thermodynamic equilibrium
- Plasma-particle interactions in mass, momentum and energy are considered in the induction zone. They are neglected in the second model. In this part the fine particles initially have the same temperature and velocity as the gas. The phase change energy at conditions where condensation occurs leads to gas temperature variations under 10 K.
- A net emission coefficient gives the radiative losses from argon and metal vapor (12).
- NH_3, H_2 and N_2 diffuse at the same rate in argon and are in chemical equilibrium.

Solution of particle growth, transport and nitridation:

Phase change of aluminum vapor occurs by homogeneous nucleation and surface condensation. The particles generated also grow by Brownian coagulation and are transported by gas convection, thermophoresis and Brownian diffusion. Ammonia reacts with the condensed aluminum at a rate controlled by its diffusion to the surface of the particle and proportional to the molar fraction of free aluminum in the particle. The rate of this reaction is assumed to be negligible at temperatures under the solidification of aluminum due to the strongly reduced inner mobility. Other assumptions are:

- Aluminum droplets are formed by homogeneous nucleation at a rate given by (13).
- The spherical particles grow by surface condensation and Brownian coagulation in the free molecular regime ($Kn < 5$). Cluster scavenging is neglected. Evaporation is only considered in the induction zone. The sticking coefficient is 1 for temperatures higher than the solidification of Al and 0 under.
- A diffusion coefficient based on the local mean volume diameter is applied over the distribution. The consideration of axial diffusion allows solutions in recirculating flows.
- The yield of nitridation is the same for all particles at a given location.

The population of particles is represented in terms of the first three integer moments (orders K= 0, 1 and 2) of the distribution based on j, the number of aluminum atoms contained in a particle as presented in (14) for the case of iron particles: $M_K = (\Sigma j^K n_j)/\rho$. n_j is the concentration of particles of size j and ρ the gas density. An additional variable is the moment or order 1 relative to the aluminum nitride molecules in the particles, $M_N = (\Sigma i_j n_j)/\rho$, i_j being the number of molecules of aluminum nitride in a particle of size j. The equations describing vapor concentration, particle size distribution and rate of nitridation are the following:

$$\vec{\nabla}\cdot(\rho\vec{u}\omega_{Al}) = \vec{\nabla}\cdot\left(\rho D_{Al}\vec{\nabla}\omega_{Al}\right) - Ij^* m_{Al} - B_1\rho(S-1)M_{2/3}m_{Al} \quad [1]$$

$$\vec{\nabla}\cdot(\rho\vec{u}M_K) = \vec{\nabla}\cdot\left(\rho\overline{D}\vec{\nabla}M_K\right) - \vec{\nabla}\cdot(\rho\vec{u}_{th}M_K) + I\left(j^*\right)^K + KB_1\rho(S-1)M_{K-1/3} + a_K\rho^2\Theta_{0,0}M^2{}_{K/2} \quad [2]$$

$$\vec{\nabla}\cdot(\rho\vec{u}M_N) = \vec{\nabla}\cdot\left(\rho\overline{D}\vec{\nabla}M_N\right) - \vec{\nabla}\cdot(\rho\vec{u}_{th}M_N) + B_{NH3}\rho M_{2/3}n_{NH3}(1-X) \quad [3]$$

In the preceding equations $\vec{u}$ is the gas velocity, ω_{Al} is the mass fraction of metal vapor, D_{Al} and $\overline{D}$ are the diffusion coefficients for aluminum and for the particles. I and j* are the nucleation rate and size, $B_1 = (36\pi)^{1/3} n_s v_{Al}^{2/3} (k_B T/2\pi m_{Al})^{1/2}$ is the surface condensation coefficient. n_S is the saturation molecular concentration of aluminum, k_B is Boltzmann's constant, T the gas temperature and m_{Al} and v_{Al} the mass and volume of one atom. S is the supersaturation ratio, a_K is a constant equal to -0.5 for K=0, 0 for K=1 and 1 for K = 2. n_{NH3} is the molecular concentration of ammonia, $\Theta_{0,0}$ is the mean Brownian collision coefficient as defined by Frenklach and Harris (15). B_{NH3} is the rate constant for the heterogenous nitridation reaction and $X = M_N/M_1$ is the molar fraction of aluminum that is nitrided in the particles.

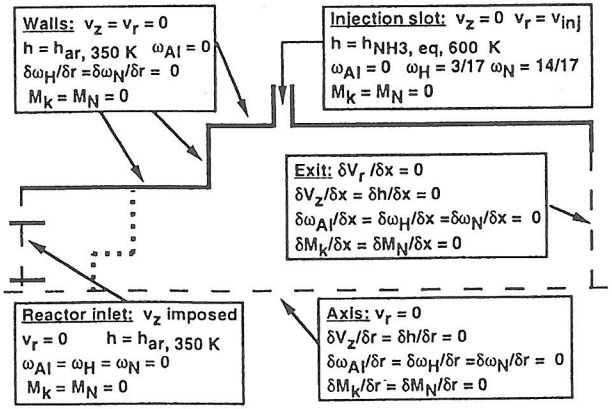

Figure 2. Boundary conditions used in the simulations

Boundary conditions and numerical techniques:

The boundary conditions used are presented in Figure 2. The entrance profiles for the velocities, temperatures and aluminum vapor concentrations in the second model are interpolated from the solution of the first model. The boundary between these two models is shown by the line with thick, short dots. At this boundary the particles injected initially are completely evaporated, and condensation of aluminum has not started. A progressive grid refining technique is used to accelerate and stabilize the solution. The solution obtained from a coarser grid is used to interpolate the initial estimates of a finer grid, for three successive grid levels. An artificial time step is adjusted according to the variation of the moments of the distribution.

3. Results:

The simulations use an induction power input of 4.5 kW at 2.9 MHz. The argon flowrate is of 27.2 slpm. The aluminum feedrate is of 0.25 mg/s and the ammonia flowrate of 3.6 slpm. Figures 3 and 4 show the fields of the temperature and the normalized stream function. An important recirculation occurs downstream of the tube enlargment. A maximum in temperature of more than 9000 K is observed. Particles are injected on the axis where temperatures are lower, but they are completely evaporated at the point of startup of the condensation model.

Figure 5 shows the field of the logarithm of the particle number concentration (m^{-3}) in the reactor and Figure 6 the mean volume diameter of particles (nm). The strong gradients near the walls of the induction tube cause the formation of fine particles in high concentrations. Particles of larger size but in lower number concentration are generated near the reactor axis, where gradients are smaller. Typically, deposition of metal vapor by diffusion and particles by thermophoresis and Brownian diffusion on the walls of the induction tube and the condensation tube account for 45% of the aluminum injected. Figure 7 presents the contour lines for the yield of the nitridation reaction. The conversion is high for intermediate values of the radius. It is low near the reactor axis. This is explained by the low specific surface of particles and the low fraction of ammonia due to the limited jet penetration and the high temperatures causing its decomposition. Conversion is also low near the walls of the condensation zone, which is explained by the assumption of negligible reaction for temperatures under the solidification of aluminum. Table 1 shows the dependance of the cup mixing averaged yield and number diameter at the exit of the reactor. A higher ammonia flowrate leads to the synthesis of finer particles and a greater yield of nitridation, within the range studied.

Table 1. Effect of the quench flowrate on exit powder properties

Ammonia flowrate (slpm)	1.8	2.4	3.6
Mean num. diameter (nm)	41	31	28
Yield	0.87	0.92	0.93

4. Conclusions:

A two-dimensional model is developed for the synthesis of aluminum nitride in an induction plasma reactor. Metal particles are generated by homogeneous nucleation and grow by surface condensation and Brownian coagulation in the free molecular regime. Aluminum particles are nitrided by a heterogeneous surface reaction with ammonia. The growth and reaction model allows for simulations in complex and recirculating flows, considering thermophoresis and Brownian diffusion in both directions. Fine particles are generated near the walls of the induction tube, where temperature gradients are important. On the axis, particles are formed further downstream and in larger sizes due to the more gradual cooling. Higher nitridation yields are estimated at intermediate values of the radius. The yield is limited by low temperatures near the walls and by low specific surface and ammonia concentration near the reactor axis. Particle and vapor deposition on the walls typically account for 45% of the injected aluminum, in the configuration studied. Increasing the ammonia flowrate leads to powders of lower size and increased yield of nitridation.

References:

(1) Kishi, M., Suzuki, M. and K. Ogawa, J. Appl. Phys. 31: 1153-1159 (1992)
(2) Lu, Z. P., Pfender, E., Proceedings ISPC-9, Pugnochiuso, Italy: 675-678 (1989)
(3) David, M., Babu, S. V. and D. H. Rasmussen A.I.Ch.E. J., 36:871-876 (1990)
(4) Ageorges, H., Chang, K., Qafssaoui, F., Megy, S., Baronnet, J.-M. and P. Roumilhac, J. High Temp. Chem. Proc. Suppl. no. 3, vol. 1: 275-281 (1992)
(5) Etemadi, K. Pl. Chem. Pl. Proc., 11:41-56 (1991)
(6) Wehling, C., Heitz, F. and H. Hausner, Proc. ISPC-10, Bochum 1.4-5 (1991)
(7) Ishizaki, K., Egashira, K., Tanaka, K. and P.B. Celis J. Mat. Sci. 24:3553 (1989)
(8) Vissokov, G. P., Brakalov, L. B. J. Mat. Sci. 18:2011-2016 (1983)
(9) Baba, K., Shohata, N. and M. Yonezawa Proc. ISPC-8, Tokyo, 2034-2039 (1987)
(10) Proulx, P., Mostaghimi, J. and M. I. Boulos Pl. Chem. Pl. Proc. 7:29-53 (1987)
(11) Mostaghimi, J. and M. I. Boulos Pl. Chem. Pl. Proc. 7:29-53 (1990)
(12) Essoltani, A., Proulx, P., Boulos, M. I., and A. Gleizes Journal of Analytical Atomic Spectroscopy 5:543-547 (1990)
(13) Girshick, S. L., and C.-P. Chiu J. Chem. Phys. 93:1273-1277 (1990)
(14) Bilodeau, J.F.and P. Proulx Aerosol Sci. Tech. to be published
(15) Frenklach, M. and S. J. Harris J. Coll. Int. Sci. 118:252-261 (1987).

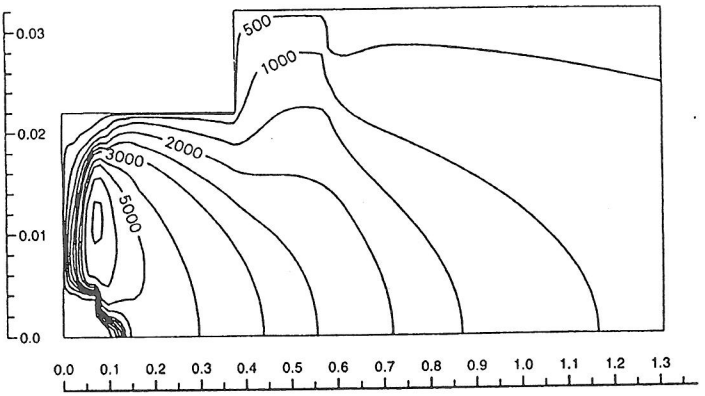

Figure 3. Temperature isocontours (K)

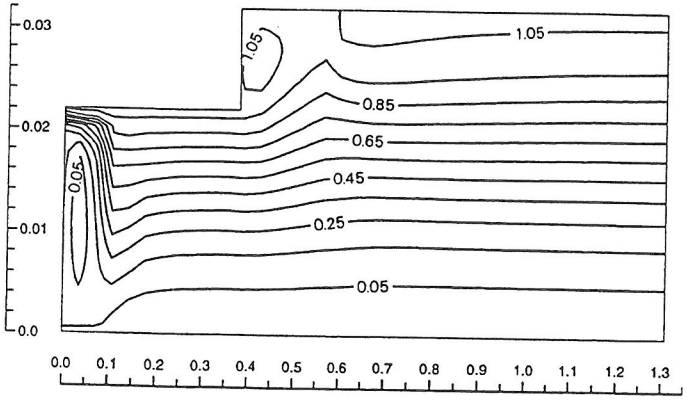

Figure 4. Stream function normalized by the total entrance flowrate

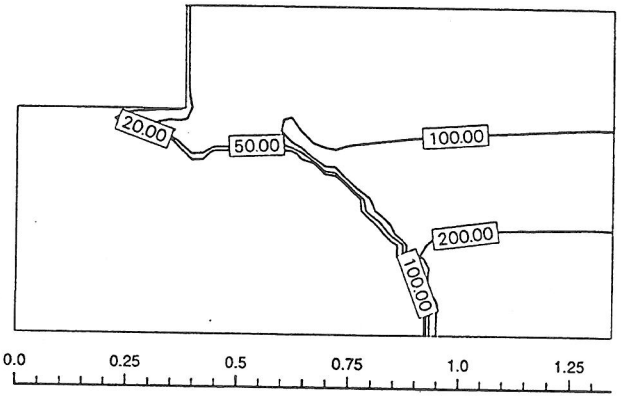

Figure 6. Mean volume diameter of particles, nm

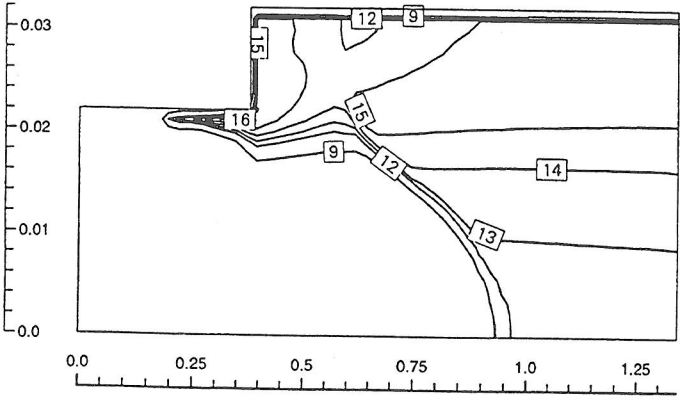

Figure 5. Logarithm of the number concentration of particles, m^{-3}

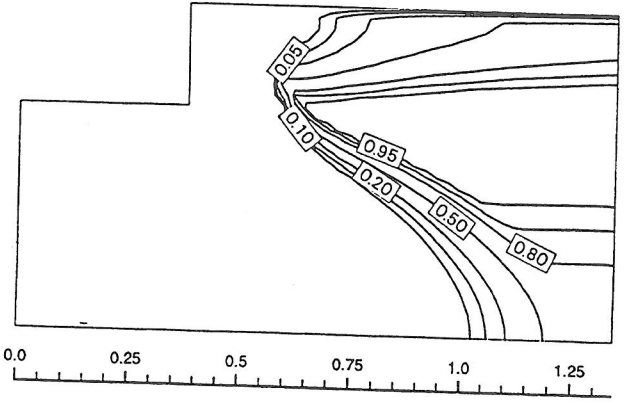

Figure 7. Molar fraction of nitrided aluminum